Deep silicon grating as high-extinction-ratio polarizing beam splitter

Jijun Feng (冯吉军)[1*], Changhe Zhou (周常河)[1,2], Bo Wang (王 博)[1], and Jiangjun Zheng (郑将军)[1]

[1] *Information Optics Lab, Shanghai Institute of Optics and Fine Mechanics, Chinese Academy of Sciences, Shanghai 201800*

[2] *State Key Laboratory of High Field Laser Physics, Shanghai Institute of Optics and Fine Mechanics, Chinese Academy of Sciences, Shanghai 201800*

[*] *E-mail: fjijun@siom.ac.cn*

Received July 18, 2008

A deep binary silicon grating as high-extinction-ratio reflective polarizing beam splitter (PBS) at the wavelength of 1550 nm is presented. The design is based on the phenomenon of total internal reflection (TIR) by using the rigorous coupled wave analysis (RCWA). The extinction ratio of the rectangular PBS grating can reach 2.5×10^5 with the optimum grating period of 397 nm and groove depth of 1.092 μm. The efficiencies of TM-polarized wave in the 0th order and TE-polarized wave in the −1st order can both reach unity at the Littrow angle. Holographic recording technology and inductively coupled plasma (ICP) etching could be used to fabricate the silicon PBS grating.

OCIS codes: 050.1950, 230.1360, 230.5440, 060.4510.

doi: 10.3788/COL20090704.0325.

Polarizing beam splitter (PBS), which plays an important role in optical communication, can split an incident beam into two orthogonally polarized light beams. The underlying principle of conventional PBSs is based on natural birefringent effects[1] or refraction effect at multilayer dielectric coatings[2]. However, the conventional multilayer film PBS is expensive due to the complicated procedure of multilayer coating. Nowadays, photonic crystal[3] as PBS has aroused more and more attention. The structure of photonic crystal is so complicated that it is difficult to be fabricated.

It seems much more interesting if a simple subwavelength grating can function as a polarizer, which has been reported in transmission[4,5], reflection[6], mold injection[7], embedded metal wire[8], and metal wire-grids[9] as broadband polarizers[10,11]. For practical use in optical communication, good extinction ratio and high efficiency with a wide angular bandwidth and a broad wavelength range are needed. Among different types of diffraction gratings, metallic reflection grating has the disadvantage of power-absorption and low damage threshold. Low-contrast dielectric grating, such as fused-silica grating, is suitable to function as transmission PBS for its low refractive index. High-contrast dielectric grating, such as silicon grating, is better to be used as total-internal-reflection (TIR) PBS grating for its high refractive index. TIR dielectric gratings can achieve diffraction efficiency as high as 100%. It was previously reported that dielectric TIR gratings with only two diffraction orders can achieve unity diffraction efficiency under the Littrow condition to generate high-efficiency reflective diffraction[12−15]. Marciante *et al.*[14] designed and fabricated a high-dispersion, high-efficiency, surface-relief diffraction grating with extremely low polarization sensitivity for L-band (1560–1610 nm) telecommunication applications.

Figure 1 depicts such a TIR grating with period Λ and groove depth h between two materials with refractive indices n_1 and n_2 ($n_1 > n_2$). In the Littrow mount, the diffracted −1st order light retraces the same path as the incident light. There will exist only two diffracted orders: the 0th and −1st orders, if the grating period Λ satisfies[13]

$$n_1 > \frac{\lambda}{2\Lambda} > n_2, \tag{1}$$

where λ is the vacuum wavelength of the light incident from material n_1.

It is known that silicon is the most common material in semiconductors. Since Tsang *et al.* fabricated the silicon grating[16], the fabrication technology and the application of silicon gratings developed rapidly. Because of the high refractive index of silicon[17], it is appropriate to utilize the TIR phenomenon of the material. Based on the phenomenon of TIR, the high-extinction-ratio reflective silicon PBS grating can be designed regardless of grating tooth shape[13−15]. Without loss of generality, a rectangular grating is considered. As shown in Fig. 1, n_1 and n_2 are refractive indices of silicon and air, respectively, and b is the ridge width. The duty cycle f

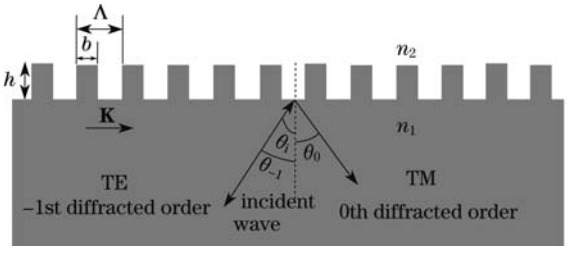

Fig. 1. Schematic illustration of a silicon TIR PBS grating. n_1 and n_2 are refractive indices of silicon and air, respectively, Λ is grating period, b is ridge width, h is depth, θ_i is incident angle (under Littrow mounting), θ_0 and θ_{-1} denote diffraction angles of the 0th and −1st orders in silicon, respectively.

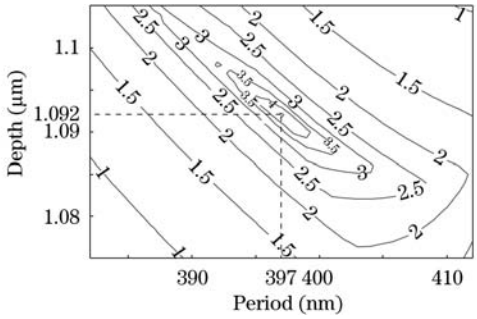

Fig. 2. Logarithm of the extinction ratio of the PBS grating for different profile parameters (under Littrow mounting). The highest extinction ratio (5.4 in logarithmic scale) occurs at the groove depth of 1.092 μm with the period of 397 nm.

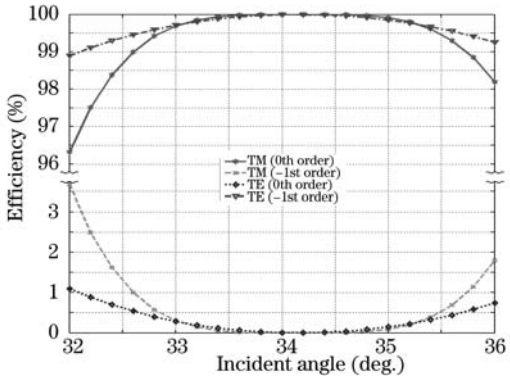

Fig. 3. Diffraction efficiency of the PBS grating as a function of incident angle (Λ = 397 nm, h = 1.092 μm).

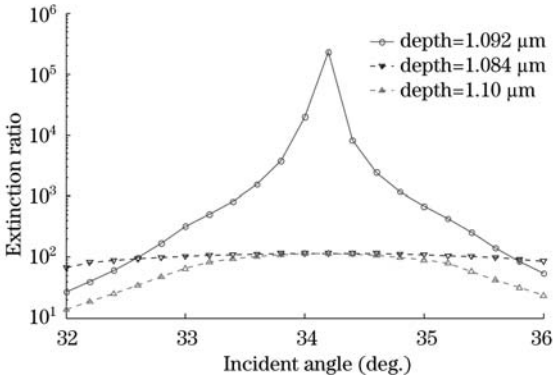

Fig. 4. Extinction ratio of the PBS grating as a function of incident angle with different groove depths (Λ = 397 nm).

is defined as the ratio of the ridge width b to the period Λ. In our design, refractive index $n_1 = 3.47694$, and $f = 0.5$. A monochromatic plane wave of wavelength λ is obliquely incident upon the grating at Littrow angle of $\theta_{\rm i} = \sin^{-1}(\lambda/\ (2n_1\Lambda))$. The TM-polarized wave (magnetic field vector perpendicular to the plane of incidence) and TE-polarized wave (electric field vector perpendicular to the plane of incidence) are diffracted in the 0th and −1st orders, respectively. Let η_k^{TX} represent the diffraction efficiency in order k for TX polarization. The extinction ratio C of the PBS grating is defined as[4]

$$C = \min\left\{\eta_0^{\rm TM}/\eta_0^{\rm TE}, \eta_{-1}^{\rm TE}/\eta_{-1}^{\rm TM}\right\}. \quad (2)$$

The grating vector **K** is assumed to lie in the plane of incidence. The diffraction properties of silicon grating can be studied at the wavelength of 1550 nm with inequality (1) by using the rigorous coupled wave analysis (RCWA)[18,19]. In Fig. 2, the contour of the logarithm of the grating extinction ratio versus grating period and groove depth is depicted with Eq. (**??**). The optimized extinction ratio can reach 2.5×10^5 with the prescribed grating period of 397 nm and groove depth of 1.092 μm at Littrow angle of 34.16°. Moreover, the efficiencies of TM-polarized wave in the 0th order and TE-polarized wave in the −1st order can both reach unity with the optimized parameters, respectively. Extinction ratio of the PBS grating will fall with deviations of period and depth from the optimum parameters as shown in Fig. 2. The extinction ratio higher than 100 can still be obtained provided that 344 nm < Λ <412 nm and 1.076 μm < h< 1.205 μm. Within ranges given above, the efficiencies of TM-polarized wave in the 0th order and TE-polarized wave in the −1st order are more than 99.05% and 99.04%, respectively.

Figure 3 reveals the diffraction efficiencies with the varying incident angle. TM- or TE-polarized wave is incident upon the designed PBS grating at the incident angle around 34.16°. In Fig. 4, the extinction ratios with different groove depths are compared. With the optimum groove depth of 1.092 μm, the extinction ratio higher than 100 can be maintained with the angle varying from 32.61° to 35.73°, which has 3.12° angular bandwidth. The efficiencies of TM-polarized wave in the 0th order and TE-polarized wave in the −1st order are more than 99.02% and 99.47%, respectively. However, with the deviation of groove depth from the optimum parameter, the angular bandwidth drops rapidly. With groove depths of 1.084 and 1.10 μm, the corresponding angular bandwidths are 2.64° (with angle varying from 32.84° to 35.48°) and 1.2° (with angle varying from 33.56° to 34.76°), respectively. Both have the maximum extinction ratio of 116 at the Littrow angle.

Wavelength selectivity of the designed grating is studied for grating with fixed incident angle of 34.16° and for grating with corresponding Littrow angle for wavelength ranging in the C+L bands, as shown in Fig. 5. Extinction ratios with different groove depths for these two gratings are shown in Fig. 6. For the grating with fixed incident angle and optimum groove depth, extinction ratio higher than 100 can be obtained for 16-nm spectral bandwidth (with the wavelength ranging from 1542 to 1558 nm). The efficiencies of TM-polarized wave in the 0th order and TE-polarized wave in the −1st order are more than 99.66% and 99.05%, respectively. With the optimized groove depth increased or decreased, the corresponding peak extinction ratios of both gratings are "red-shifted" or "blue-shifted". This phenomenon can be well explained by the modal theory[20,21]. The grating mode can accumulate a phase shift of

$$\Delta\varphi = \frac{2\pi}{\lambda}\hat{n}_{\rm eff}h, \quad (3)$$

where $\hat{n}_{\rm eff}$ is the effective index of the grating mode. The deeper groove depth h is corresponding to the larger incident wavelength λ for the peak extinction ratio in Fig. 6.

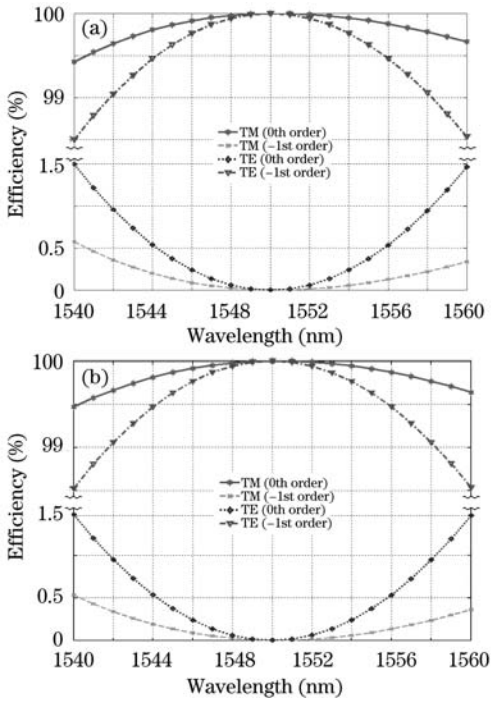

Fig. 5. Diffraction efficiency of the PBS grating as a function of incident wavelength (a) with fixed incident angle of 34.16° and (b) with corresponding Littrow angle for each wavelength.

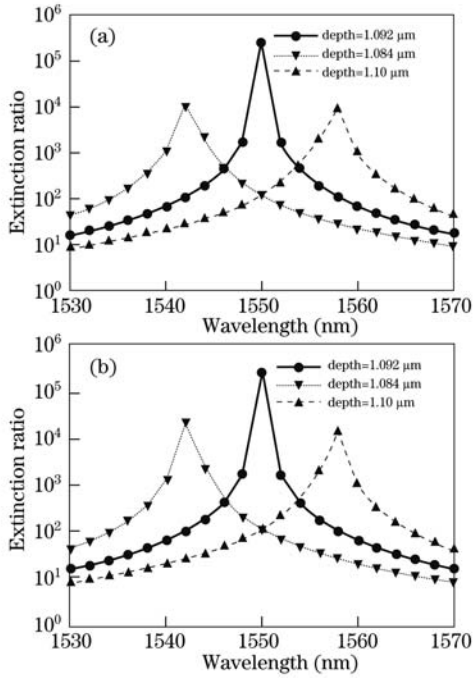

Fig. 6. Extinction ratio of the PBS grating as a function of incident wavelength with different groove depth (a) with fixed incident angle of 34.16° and (b) with corresponding Littrow angle for each wavelength.

The high-density silicon TIR grating can be fabricated by using holographic interference recording and ICP etching technology[22]. Holographic recording is an effective method to form a high-density grating, and ICP technology is an important dry etching method to obtain a rectangular grating with high aspect ratio. Silicon is widely used in semiconductor industry and its fabrication is compatible with the process of microelectronics and micromachining. It should be mentioned that the actual profile of the binary silicon grating might be trapezoidal after etching. In fact, the conditions that define the TIR grating are valid regardless of the nature of the grating profile[13−15].

Figure 7 shows that the logarithm of the extinction ratio higher than 100 can be tolerated with the groove depth between 1.084 and 1.10 μm around the optimum groove depth of 1.092 μm as well as the duty cycle within the range from 0.478 to 0.516 around the prescribed duty cycle of 0.5. This corresponds to a deviation of 1% from the optimum groove depth and more than 3% from the optimum duty cycle. These are useful guidelines to fabricate a successful PBS grating with acceptable fabrication tolerances. However, the small tolerance of the groove depth would still make the fabrication of this kind of high-aspect-ratio and high-density silicon grating challenging.

For practical application of the PBS grating, the performance may be degraded over time as a result of moisture, particles, or pollution on the surface. However, one can cover a film over the TIR grating surface for protection from the environment. This coating is not in the optical path of the beams and thus has little influence on the performance of the grating. Another concern is the high temperature dependence of the coefficient of thermal expansion (CTE) and refractive index of silicon. However, under stable environment temperature, the grating would change little and still be very stable.

Since the light needs to be coupled into/out the silicon grating, the high refractive index of silicon should be taken into account. Some measures must be taken, for example via a silicon prism[14]. If the light is incident normally on the silicon from the air, about 31% of incident power will be reflected back by the incident interface of silicon and air. Therefore, anti-reflection measures should be considered. In order to split the TE-polarized wave (−1st diffractive order) away from the incident light for practical application, a beam splitter is needed. This would further reduce the actual efficiency. However, it should be noted that high extinction ratio can still be obtained in spite of the reduced efficiency. The extinction ratio is more important in some practical

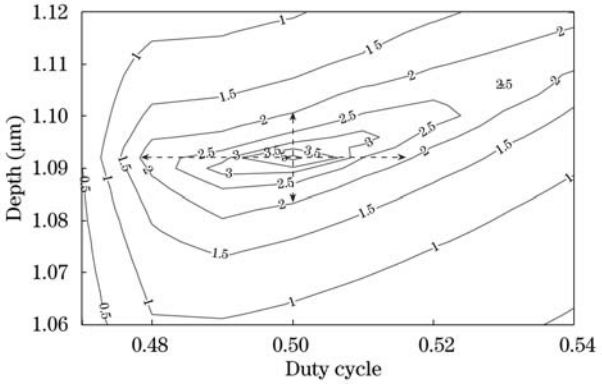

Fig. 7. Fabrication tolerances. Logarithm of the extinction ratio for different duty cycles and groove depths (under Littrow mounting, Λ = 397 nm). The extinction ratio higher than 100 is achieved if the duty cycle ranges from 0.478 to 0.516 and the groove depth is between 1.084 and 1.10 μm.

applications. So the silicon TIR grating would still be a useful PBS for practical applications in optical communication.

In summary, a deep binary silicon TIR grating has been described as a high-extinction-ratio PBS. With the optimum grating period of 397 nm and depth of 1.092 μm, the PBS grating exhibits high extinction ratio of 2.5×10^5, and the high efficiencies of TM-polarized wave in the 0th order and TE-polarized wave in the -1st order are both unity at Littrow angle. Angular bandwidth of 3.12° can be obtained for the extinction ratio higher than 100. The grating has a bandwidth of 16 nm around the wavelength of 1550 nm. Deviations of 1% from the optimum groove depth and more than 3% from the optimum duty cycle can be tolerated for grating fabrication.

The authors acknowledge the support of the National Natural Science Foundation of China (No. 60878035) and Shanghai Science and Technology Committee (No. 07SA14).

References

1. J. Li, H. Luo, Y. Guo, F. Gao, and X. Yao, Acta Opt. Sin. (in Chinese) **27,** 2027 (2007).
2. X. Fu, K. Yi, J. Shao, and Z. Fan, Chin. Opt. Lett. **6,** 544 (2008).
3. L. Wu, M. Mazilu, J.-F. Gallet, T. F. Krauss, A. Jugessur, and R. M. De La Rue, Opt. Lett. **29,** 1620 (2004).
4. B. Wang, C. Zhou, S. Wang, and J. Feng, Opt. Lett. **32,** 1299 (2007).
5. C. Zhou, B. Wang, J. Feng, and H. Ru, Laser Optoelectron. Prog. (in Chinese) **45,** (2) 18 (2008).
6. D. Delbeke, R. Baets, and P. Muys, Appl. Opt. **43,** 6157 (2004).
7. E. J. de Carvalho, E. da Silva Braga, and L. H. Cescato, Appl. Opt. **45,** 100 (2006).
8. L. Zhou and W. Liu, Opt. Lett. **30,** 1434 (2005).
9. Y. Ekinci, H. H. Solak, C. David, and H. Sigg, Opt. Express **14,** 2323 (2006).
10. L. Zhang, C. Li, W. Liu, L. Zhou, G. Wu, and D. Wang, Acta Opt. Sin. (in Chinese) **26,** 1048 (2006).
11. Z. Y. Yang and Y. F. Lu, Opt. Express **15,** 9510 (2007).
12. E. Popov, L. Mashev, and D. Maystre, Opt. Commun. **65,** 97 (1988).
13. J. R. Marciante and D. H. Raguin, Opt. Lett. **29,** 542 (2004).
14. J. R. Marciante, J. I. Hirsh, D. H. Raguin, and E. T. Prince, J. Opt. Soc. Am. A **22,** 299 (2005).
15. Y. Zhang and C. Zhou, J. Opt. Soc. Am. A **22,** 331 (2005).
16. W.-T. Tsang and S. Wang, J. Appl. Phys. **46,** 2163 (1975).
17. J. Feng, C. Zhou, B. Wang, and H. Ru, Proc. SPIE **6832,** 68320S (2007).
18. M. G. Moharam, E. B. Grann, D. A. Pommet, and T. K. Gaylord, J. Opt. Soc. Am. A **12,** 1068 (1995).
19. P. Lalanne and G. M. Morris, J. Opt. Soc. Am. A **13,** 779 (1996).
20. A. V. Tishchenko, Opt. Quantum Electron. **37,** 309 (2005).
21. T. Clausnitzer, T. Kämpfe, E.-B. Kley, A. Tünnermann, A. Tishchenko, and O. Parriaux, Appl. Opt. **46,** 819 (2007).
22. S. Wang, C. Zhou, H. Ru, and Y. Zhang, Appl. Opt. **44,** 4429 (2005).